Water dynamics explored by femtosecond infrared spectroscopy

Yeremenko, Sergiy

Chapter 6

Dynamical Stokes shift and anharmonicity of the OH-stretch vibration in water molecules

Abstract

In this Chapter, we address the issue of the presence of the Stokes shift in the spectrum of the OH-stretch vibration of water. We also elucidate the value of the anharmonicity of this vibrational mode. The method of frequency resolved pump-probe is used. Analysis of the experimental data shows that within an experimental uncertainty of the order of 5 cm^{-1} the observed spectral dynamics is related only to the thermal effect, i.e. a modification of the absorption spectrum caused by heating of the sample due to absorption of the pump pulse energy. No appreciable Stokes shift is detected. The shape of the transient spectra is analyzed performing a global fit of the linear absorption and pump-probe spectra. The frequency shift between the transitions $|g\rangle \rightarrow |e\rangle$ and $|e\rangle \rightarrow |2e\rangle$, which is determined by the anharmonicity of the corresponding vibrational mode, amounts to 190±20 cm^{-1}. The width of the line corresponding to the $|e\rangle \rightarrow |2e\rangle$ vibrational transition is found to be approximately 1.3-1.5 times larger than the width of the fundamental $|g\rangle \rightarrow |e\rangle$ transition, while their height ratio is close to the value 1.4. Frequency-resolved pump-probe experiments on solutions of water in acetonitrile substantiate the validity of our conclusions on pure water.

Part of the work as presented in this Chapter is covered by the following paper:

S. Yeremenko, M.S. Pshenichnikov, and D.A. Wiersma. “Dynamical Stokes shift of the OH-stretch vibration in water molecules”, in preparation (2004)

6.1 Introduction

Water is often called the "solvent of life" since most chemical and biological processes take place in this medium. Moreover, in many cases water participates in these processes largely determining the effect. In spite of considerable research efforts, the properties of water and its role in life processes are still not completely understood. In this respect the solvation dynamics, i.e. the time-dependent interactions of the solvent and solute, are of primary interest. However, comprehension of the solvation dynamics in water is very difficult without knowledge of the dynamic properties of the pure solvent. It has been shown, that spectroscopic methods are informative tools for studying liquid state dynamics [1-8]. Infrared (IR) spectroscopy was proven to be an efficient technique for the investigation of the microscopic molecular dynamics of liquid water, since the molecular vibrations can be used as very sensitive probes of the dynamics of the microscopic structure [5,9-11].

One of the key spectroscopic parameters is the so-called Stokes shift, which is the difference in the average frequency of the relaxed emission (fluorescence) and the linear absorption. Upon excitation of the vibrational transition, the environment of the probe molecule responds to the new state of the chromophore, which consecutively leads to a shift of the frequency of the excited vibrational mode to lower values. Hence, the Stokes shift is caused by the difference in the interaction of the chromophore with the environment (solvent) in the ground and excited states. Since the response of the solvent is not instantaneous, the Stokes shift also evolves in time. The dynamics of the Stokes shift is determined by the character of the molecular motions and intermolecular interactions in the system. The value of the Stokes shift is an essential parameter in the model describing the system-bath interactions (see Chapter 3). The line shape function, which is a key parameter unifying linear and nonlinear spectroscopic experiments, becomes complex if the Stokes shift is present (Eq.3.40 in Chapter 3).

It has been shown that the OH-stretch vibration of water molecules is sensitive to hydrogen bonding, whereas the latter phenomenon mostly determines the microscopic structure and dynamics of water [12-24]. Therefore, in most studies this vibrational mode is used as a probe for the investigation of the dynamics of the water structure [5,9-11,25-29]. Several theoretical and experimental studies have addressed the Stokes shift of the OH-stretch vibration frequency of water molecules in the liquid phase. A solution of HDO in heavy water is usually employed in these studies as a convenient experimental system (see Chapter 1). In hole burning experiments on the OH-stretch vibration (spectrum of HDO molecules dissolved in D_2O) no appreciable Stokes shift was observed [5,9]. In this study, the spectral dynamics were presented in terms of the first moment of the transient spectrum. The symmetric behavior of the first moment for the case of the excitation on the red and blue wings of the absorption line provides a straightforward indication of the absence of a considerable Stokes shift.

However, in later measurements a (very) pronounced Stokes shift (~74 cm^{-1}) occurring on the timescale of the order of 500 fs was found in the same system. In the latter study a two-color pump-probe (PP) technique was employed [1]. The excitation and probing were performed on the red and blue side of the absorption spectrum, respectively and vice versa. The Stokes shift and its dynamics were inferred from the initial behavior of the pump-probe signals measured with these two combinations of excitation and probing wavelength. The physical origin of the Stokes shift was explained by the effect of strong coupling of the OH-stretching mode to the hydrogen bond, leading to a substantial difference between the potential energy functions of the hydrogen bond for the ground and excited state of the OH-stretching mode. Recently in MD simulations, employing a semiclassical approach and specially dedicated to model the spectroscopic characteristics of this system, the value of the

Stokes shift was estimated to be on the order of 57 cm^{-1} [30]. The latter value is in good agreement with the value calculated according to the following expression

$$\lambda = \frac{\Delta^2 \hbar}{2k_B T} \tag{6.1}$$

This expression is derived from Eq.3.30 and 3.31 (Chapter 3) assuming that $\hbar\omega >> 2k_B T$, which is usually called the high temperature limit. In the latter theoretical study, the dynamics of the Stokes shift was predicted to be bimodal with a fast timescale of the order of 30 fs and a slow one in the range of 700 fs.

Thus, the existence of a Stokes shift for the OH-stretching vibrational mode in liquid water, its value, and the timescale of corresponding dynamics still remain controversial issues. The experimental methods employed to date, to study the Stokes shift on this vibration, had a rather restricted time-frequency resolution. All these experiments were performed with relatively long IR pulses (with a duration in the range of 150-250 fs) having a spectrum substantially narrower than the absorption spectrum of the chromophore. Therefore, in such experiments the frequency of the probe has to be changed during the experiment, which can substantially lower the accuracy of the experimental data. Sub-100 fs IR pulses with a spectrum covering simultaneously the range of both the $|g\rangle \rightarrow |e\rangle$ and $|e\rangle \rightarrow |2e\rangle$ vibrational transitions of the OH-stretching mode of HDO, are required to perform frequency resolved pump-probe measurements without tuning the laser wavelength during the experiment. This provides maximal precision and consistency of detection of the spectral dynamics.

The second important issue, considering nonlinear IR spectroscopy on water, is the parameters of the excited state absorption of the OH-stretch vibration. It has been shown that the frequency shift between the ground and excited state transitions, which is determined by the anharmonicity of the vibration, is comparable with the width of the corresponding absorption band. Its value, as generally accepted nowadays [1,11,25,31], is of the order of 270 cm^{-1}. Consequently, the excited state absorption is involved in the interaction with the laser pulses. Therefore, for a correct interpretation of the experimental results both $|g\rangle \rightarrow |e\rangle$ and $|e\rangle \rightarrow |2e\rangle$ vibrational transitions have to be taken into account in the analysis of the experimental data.

The value of the anharmonicity of the OH-stretching vibrational mode was found in early pump-probe experiments on a solution of HDO in D_2O [32]. It was later used without further verification, in most of the ultrafast IR studies of water [1,31]. The anharmonicity was derived as a frequency shift between the peak maxima of the induced bleaching and induced absorption in the pump-probe spectrum. However, when the width of the spectral bands is comparable to the value of the anharmonicity, the positions of the peaks in the pump-probe signal do not correspond directly to the peak positions of respective spectral bands. This can be explained by a simple illustration presented in Fig.6.1. In Fig.6.1(a) a model pump-probe spectrum is depicted as a solid line and the corresponding spectral bands shown as dashed and short-dashed lines. As one can see, due to the strong overlap between the spectral bands related to the ground and excited state transitions, the peaks of the pump-probe signal substantially deviate from the peaks of the corresponding spectral bands. In order to make a quantitative estimation of this deviation, we performed the following simulation. The pump-probe signal was modeled as the difference of two identical Gaussian bands: one related to the induced absorption and the other to the induced bleaching.

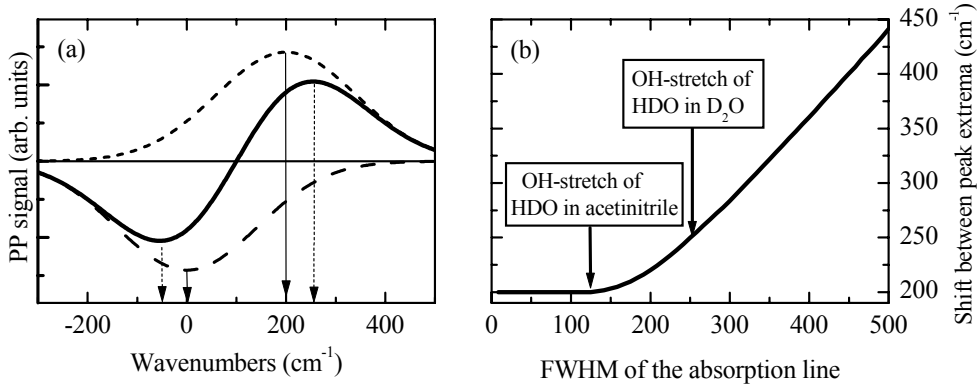

Fig.6.1. A model pump-probe spectrum with corresponding spectral bands (a). The arrows depict the positions of the peak maxima. The ground and excited state transitions spectral bands are shown as short dashed and dashed lines respectively. The shift between the maxima of the pump-probe peaks as a function of the full width at half maximum of the spectral bands for an anharmonicity of 200 cm^{-1} is shown in (b).

$$S(\omega) = \exp\left[-(\omega-\Delta)^2/\sigma^2\right] - \exp\left[-\omega^2/\sigma^2\right] \tag{6.2}$$

where σ determines the width of the peak and Δ – the anharmonicity. Taking the derivative of this expression with respect to the wavelength, equating the result to zero and solving this equation numerically, we obtain the positions of extrema of the pump-probe signal. The shift between the maxima of the peaks of the pump-probe signal versus the full width at half maximum of the spectral band for the anharmonicity of 200 cm^{-1}, is shown in Fig.6.1b. In this case, the frequency shift between the peaks of the pump-probe signals corresponds to the real anharmonicity, when the width of the spectral bands does not exceed 150 cm^{-1}, substantially increasing with further broadening of the spectrum. The spectrum of the OH-stretching mode of HDO in heavy water has a width of approximately ~250 cm^{-1}, which is substantially beyond the regime of direct correspondence of the pump-probe peaks positions to the positions of the maxima of the corresponding spectral bands. It is necessary to note, that in the simulations presented here we assumed that the spectral bands corresponding to the ground and excited state transitions have identical shape and intensity. This assumption may not be completely justified in practice. For example, previous pump-probe experiments on the spectrum of the OH-stretch vibration of HDO in heavy water indicated that the width of the overtone state transition is considerably larger than the width of the fundamental transition [25,33]. In this case our simulations slightly underestimate the extent of the regime of the direct correspondence of the peaks in the pump-probe signal and the real spectral bands. Thus, in order to find the anharmonicity of the OH-stretching mode of HDO in heavy water, a simple observation of the frequency shift between the extrema of the pump-probe signal is not sufficient. Further analysis of the experimental pump-probe data is required.

In this Chapter we study the dynamical Stokes shift of the OH-stretch vibration of HDO dissolved in D_2O using the frequency resolved pump-probe technique. Also, pump-probe experiments on solutions of HDO and H_2O molecules in acetonitrile were performed, in order to clarify the characteristics of the excited state absorption of the OH-stretch vibration and to find the anharmonicity of this vibrational mode. We show that within the accuracy of our

experiment, which is of the order of 5 cm^{-1}, no Stokes shift can be detected. The frequency shift between the ground and excited state transitions is found to be 190±20cm^{-1}.

6.2 Experiment

The observation of the Stokes shift of the OH-stretching vibrational mode of water by measuring the relaxed fluorescence spectrum is practically impossible, since in water the radiationless vibrational energy relaxation channels are very effective [29,34,35]. Accordingly, the fluorescence quantum yield is low. In this case pump-probe turns out to be the most suitable method to determine the Stokes shift. Furthermore, this method provides a dynamic picture of the relaxation process [25].

To carry out the experiments, IR pulses of ~70 fs duration, with energies of about 10 μJ and tunable in the range 2800 – 4000 cm^{-1} , were generated at a 1 kHz repetition rate using a home-built 3-stage optical parametric amplifier (OPA). The method of generation and characterization of the IR pulses, employed in this experiment is described in detail in Chapter 2.

The experimental setup for carrying out pump-probe experiments is depicted and discussed in detail in Chapter 2; in Fig.6.2 we present only its general scheme. For the pump-probe experiments, the IR output of the optical parametric amplifier is split into two parts, constituting the pump and probe pulses. One pulse can be delayed with respect to the other one by means of a precisely controlled scanning delay stage. The pump and probe beams are focused into the sample and recollimated with two spherical 10 cm mirrors. The probe was spectrally dispersed through a monochromator (CVI) and its spectral components measured with a liquid-nitrogen cooled InSb detector (Hamamatsu). A synchronous 500 Hz chopper was inserted in the pump beam. The pump-probe signal (modulation of the probe beam intensity ΔI^{probe}) was processed with a lock-in amplifier, while the reference signal (the probe beam intensity I^{probe}) was simultaneously detected as the DC component of the detector output. Both signals were digitized and stored in a computer. The difference absorption signal (in units of Δ O.D.) was calculated as the ratio $\Delta I^{probe}/ I^{probe}$. The experiments were performed with the

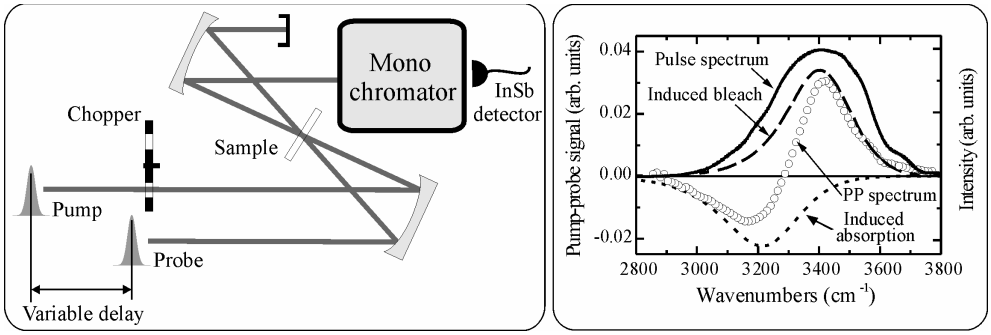

Fig.6.2. Schematic of the setup for pump-probe experiments (left panel). In the right panel the spectrum of the laser pulses (thick solid line) is shown along with the pump-probe spectrum of the OH-stretching vibration of HDO in D_2O (open circles). The dashed and dotted lines in the right panel depict the components of the pump-probe spectrum: induced bleaching and induced absorption, respectively.

polarization of the pump and probe pulses set at 54.7°, which provides the signal free of orientational anisotropy [36].

The spectrum of 70 fs laser pulses covers both $|g\rangle \rightarrow |e\rangle$ and $|e\rangle \rightarrow |2e\rangle$ vibrational transition regions as shown on the right hand side of Fig.6.2. At this figure the laser spectrum is depicted as a thick solid line, while the pump-probe spectrum of our sample and its components are shown as open circles, dashed and dotted lines respectively. Employing such broadband excitation spectrum and short pulse duration, enables us to measure the pump-probe signal throughout the entire region of 2900-3700 cm^{-1} without tuning the wavelength of the laser output during the experiment. This allows the recording of very accurate transient pump-probe spectra with high spectral and temporal resolution.

Three types of samples were studied: a solution of HDO in D_2O, H_2O in acetonitrile and a mixture of HDO, H_2O and D_2O molecules in acetonitrile. In the first two samples the concentration of HDO in D_2O and H_2O in acetonitrile was approximately 1 molar percent (0.6 M). In the third sample the total concentration of water molecules (HDO, H_2O and D_2O) in acetonitrile was 5 molar percent. In the last sample the equilibrium concentration of HDO exceeded the concentration of H_2O by approximately a factor of seven. The optical density of the sample at the peak of OH-stretching absorption line was for all the samples in the range 0.5-0.6. The solution was pumped through a sapphire nozzle to form a free-standing jet of 100μm thickness.

6.3. Experimental results and discussion

6.3.1 The vibrational Stokes shift

In order to study the spectral dynamics and determine a possible Stokes shift for the OH-stretch vibration of HDO dissolved in D_2O we performed a series of frequency-resolved

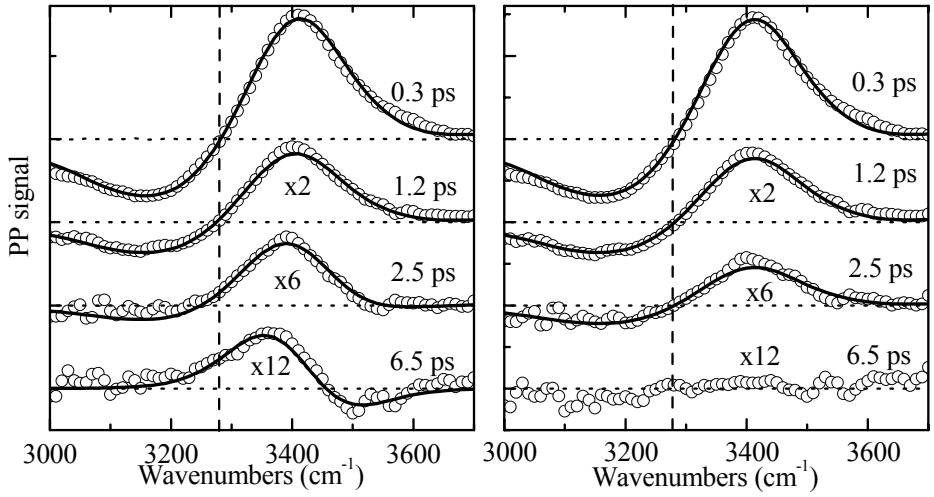

Fig. 6.3. Frequency-resolved pump-probe signals as measured in the experiment (left panel, open circles) and after the thermal pump-probe signal has been subtracted (right panel, open circles). The solid lines represent numerical simulations according to the model described in the text.

pump-probe measurements on the corresponding vibrational spectrum. The experimental pump-probe signals for four representative delays (0.3, 1.2, 2.5 and 6.5 ps) are shown in Fig.6.3a as open circles. The transient pump-probe spectra consist of an induced bleaching (shown as positive signal) and an induced absorption (negative signal). As one can see the shape of the pump-probe signal contour is slightly altered when the delay between the excitation pulses is increased. The changes in the spectrum become noticeable approximately at a delay of 1 ps. With increasing delay between pump and probe pulses the position of the maximum of the induced bleaching signal shifts to lower frequencies, while the relative amplitude of the induced absorption decreases.

In the situation where the excited state absorption makes an appreciable contribution to the signal, and a direct analysis of the contour behavior is complicated, the behavior of the zero crossing frequency can be used as a very sensitive indicator of the spectral dynamics. The zero crossing frequency is the point at which the pump-probe spectrum has zero intensity changing from the induced bleach to the induced absorption. The zero crossing frequency extracted from our experimental pump-probe signals is depicted in Fig.6.4 as open triangles. This value was found by performing a linear fit to several experimental points around the zero signal intensity (approximately in the range ±20 cm^{-1}) for each experimental transient spectrum. Such a procedure provides more reliable data with respect to the signal noise than the direct use of the experimental point corresponding to the signal with the lowest amplitude.

As one can see, the zero crossing point does not move appreciably up to 1 ps, shifting gradually to lower frequencies with further increase of the delay between the pulses. Near a delay of 4 ps it settles to a constant value shifted from the initial position by almost 100 cm^{-1}.

We have shown in Chapter 5 that the pump-probe signal has a noticeable thermal component, which originates from the changes in the position, intensity and width of the

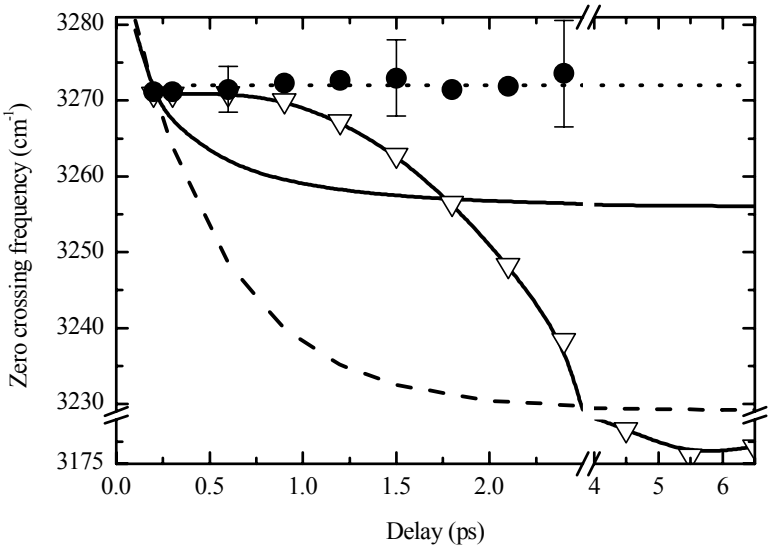

Fig. 6.4. Zero-crossing point for experimental frequency resolved pump-probe signals (empty triangles) and after the thermal pump-probe signal has been subtracted (solid circles). The thin solid and dotted lines are drawn as eye guides. Solid and dash lines represent numerical simulation of the zero-crossing point behavior for the Brownian oscillator model with the parameters described in the text.

absorption spectrum, as a result of a temperature rise in the focal volume of the sample. The temperature change in the sample is caused by the energy of an excitation pulse absorbed by the chromophore and the solvent and dissipated in the sample after vibrational relaxation. The pump-probe signal at a 6.5 ps delay represents practically a purely thermal effect. Its shape and intensity do not change with further increase of the delay between the excitation pulses in the experimentally accessible region.

At short delays the bleaching part of the pump-probe spectrum is related to the pump-induced "hole" in the ground state and stimulated emission from the exited state, i.e. it characterizes the transition $|g\rangle \rightarrow |e\rangle$. The negative part of this signal represents the pump-induced absorption from the excited state to the higher vibrational level and, therefore, corresponds to the transition $|e\rangle \rightarrow |2e\rangle$. At large delays between the pump and the probe pulses the signal is determined by the thermal shift of the ground state of the OH-stretching vibrational transition. Thus, it represents the difference between the absorption spectra at the initial and elevated temperature.

Since the thermal effect is additive, the corresponding thermal pump-probe signal can be subtracted from the experimental data to obtain the data unaltered by the temperature shift. The PP spectra free of the thermal effect are presented in Fig.6.3b. The scaling of the thermal pump-probe spectrum was performed according to the known thermalization dynamics of this contribution (see Fig.5.12 in Chapter 5). The zero-crossing frequency for the experimental signals with the thermal contributions subtracted is shown in Fig.6.4 as solid circles. In this case, within the experimental uncertainty, the shape of the PP spectra as well as the position of the zero crossing frequency are not changed with increasing of the delay between the pulses. The fact that neither the signal shape nor the zero crossing frequency vary with a frequency change, strongly indicates the absence of the Stokes shift in this system.

Applying the theoretical formalism, summarized in Chapter 3, and the model for the thermal effects, described in Chapter 5, we can simulate the pump-probe spectra for both situations: with the thermal contribution included and with the thermal contribution subtracted. In order to simplify the representation of the experimental results we do not consider the separation of the spectrum into sub-bands corresponding to the hydrogen bonded and non hydrogen-bonded OH-oscillators (see Chapter 4 for details). The stochastic model for the description of the system-bath interactions is assumed. The correlation function is bi-exponential as introduced in Chapter 4 (see Eq.4.5) with the following parameters: $1/\Lambda_1$=130 fs, Δ_1=90 cm^{-1} , $1/\Lambda_2$=700 fs, Δ_1=65 cm^{-1}. Note, that the Stokes shift is not included in this model. The parameters of the excited state absorption used in this simulation are discussed in the next section. Simulated pump-probe spectra are presented in Fig.6.3 as solid lines. They describe the experimental data very well. The slight mismatch between the experimental and simulated data at the high-frequency side of the spectrum is due to the use of the simplified model with a single spectral band. The small divergence at the low-frequency side is related to the fact that the model implies a symmetric spectral band, while the absorption contour of the OH-stretching mode of water molecules in liquid phase is slightly asymmetric (see Chapter 4 for details).

For comparison, we have also performed numerical simulations with the Brownian Oscillator Model where the Stokes shift is taken into account (see Chapter 3, Eqs.3.38-3.42). Two overdamped Brownian oscillators were employed as an extension of the stochastic model presented above. The line-shape function in this case has the following form:

$$\begin{aligned} g(t) = &\left(\Delta_1/\Lambda_1\right)^2\left[\exp(-\Lambda_1 t)+\Lambda_1 t-1\right]-i(\lambda_1/\Lambda_1)\left[\exp(-\Lambda_1 t)+\Lambda_1 t-1\right]+ \\ &+\left(\Delta_2/\Lambda_2\right)^2\left[\exp(-\Lambda_2 t)+\Lambda_2 t-1\right]-i(\lambda_2/\Lambda_2)\left[\exp(-\Lambda_2 t)+\Lambda_2 t-1\right] \end{aligned} \tag{6.3}$$

where the parameter 2λ determines the Stokes shift. The value of the Stokes shift for every of the two parts was calculated according to the high-temperature limit approximation (Eq.6.1). The zero crossing frequency behavior calculated for the case when the fast part of the correlation function is derived from the low-frequency Raman spectrum of the solvent, that is D_2O, is shown in Fig.6.4 as a solid line. As we have shown in Chapter 4, the low-frequency Raman spectrum reflects the real spectral density of the bath modes. The value of the Stokes shift derived in these calculations perfectly matches the one computed according to the high temperature limit, which prove the validity of the high temperature approximation for this case. The other parameters of the oscillators were the same as used in previous simulations, where the stochastic model was employed. The dashed line depicts the position of the zero-crossing point for the Brownian Oscillator Model with a single exponential correlation function having a decay time of 500 fs. In the latter case the value of the Stokes shift was 74 cm^{-1} as suggested in Ref.[1]. For convenience of comparison of the experimental data and the results of our simulations, the positions of the zero crossing point found from the simulations were slightly adjusted with respect to the experimental data by shifting all the values at once along the frequency axis to match the first experimental point at 200 fs delay. This shift did non exceed 5 cm^{-1}, which is within the accuracy of the experimental data. As one can see in both situations the behavior of the zero crossing point found in the simulations is considerably different in comparison to the experimental results. Obviously, both models, where the Stokes shift is included, are not capable of describing the experimental data.

A possible explanation of the disagreement between our conclusions and the results presented in the Ref.[1] on the existence of a Stokes shift for the OH-stretching vibrational mode of HDO in heavy water is given in the Appendix 6.A1. Briefly: simulations of the two-color pump-probe experiment presented in the Ref.[1] by applying the complete theoretical formalism for the calculation of the third order nonlinear response (described in Chapter 3) show that these experimental data can be perfectly reproduced with a stochastic model, where a Stokes shift is absent. The initial behavior of the pump-probe signals interpreted in the Ref.[1] as evidence for the existence of the Stokes shift is likely to be related to the interaction of different components of the PP signal in the pulse overlap region.

Thus, our experiments have shown the absence of a considerable Stokes shift for the OH-stretch vibration of water molecules in liquid phase. The excitation of this vibrational mode does not lead to a significant reorganization of its environment and subsequent modification of the OH-bond potential. A reorganization of the adjacent hydrogen bond that takes place after excitation of the vibrational mode apparently does not induce any significant change of the OH-bond potential.

6.3.2 Characterization of the excited state transition

In the previous section, we have shown that no spectral dynamics was observed in the frequency-resolved PP at small delays, where the thermal effect is minor. Therefore, the shape of the PP spectra can be directly analyzed to extract the parameters of the exited state absorption and the anharmonicity of this vibrational mode. However, as we have discussed in Introduction, determination of the anharmonicity of the OH-stretching mode is complicated, due to the substantial broadening of the vibrational spectrum and consequent by strong overlap of the spectral bands corresponding to the $|g\rangle \rightarrow |e\rangle$ and $|e\rangle \rightarrow |2e\rangle$ transitions. In order to overcome this problem and acquire more consistent data, we have also performed frequency-

resolved pump-probe measurements on a solution of water in acetonitrile. In this case the peaks in the pump-probe spectrum should closely resemble corresponding spectral bands (see Fig.6.1b) since the spectrum of the OH-stretching mode in an acetonitrile solution is substantially narrower than in pure water.

The interaction between water molecules leading to the formation of a 3D hydrogen bond network is absent in dilute acetonitrile solutions, which substantially simplifies the system. The narrowing and the blue shift of the absorption spectrum of water in acetonitrile reflect this simplification. However, the anharmonicity of the OH-stretching mode of water is not expected to differ significantly in acetonitrile and pure water, since rather strong hydrogen bonding between water and acetonitrile molecules is present [37]. Therefore, studying dilute solutions of water in acetonitrile can provide more detailed information about the spectroscopic characteristics of water molecules in the liquid phase, especially with regard to the value of the Stokes shift. In Chapter 8, we will show that this solution also provides a convenient system to study the mechanism of energy relaxation in water.

The results of pump-probe experiments on pure water and acetonitrile solutions are presented in Fig.6.5. The pump-probe spectra (open circles) are shown with the corresponding linear absorption spectra (open squares) for three studied samples: HDO in D_2O (Fig.6.5a), HDO in acetonitrile (Fig.6.5b) and H_2O in acetonitrile (Fig.6.5c). Pump-probe spectra, shown in Fig.6.5a-c and analyzed here were measured at a delay of 500 fs between the pump and the probe pulses to assure the absence of any pulse overlap effects in the signals. In the case of a mixture of HDO, H_2O and acetonitrile (Fig.6.5b) the signal, originating from H_2O, was subtracted from the total pump-probe signal, which provides the contribution from HDO molecules only.

The peak of the induced bleaching corresponding to the ground state absorption of the OH-stretching vibrational mode of HDO molecules in heavy water, is centered at ~3420 cm^{-1}, while the peak of the induced absorption (excited state transition) related to this mode is situated at ~3170 cm^{-1} (Fig.6.5a). Thus, the frequency shift between these extrema is indeed of the order of 250 cm^{-1}. However, as we have shown in Introduction, this number does not necessarily reflect the value of the anharmonicity of the vibrational mode.

When HDO is dissolved in acetonitrile (in accordance with the blue shift of the corresponding linear absorption spectrum), the induced bleaching is positioned at ~3575 cm^{-1}, whereas the induced absorption is centered at ~3380 cm^{-1} (Fig.6.5(b)). In this case the frequency shift between the minimum and the maximum of the pump-probe spectrum equals 195 cm^{-1}, which is considerably lower than in pure water. Due to the relatively small width of the spectral bands in this situation, the magnitude of the frequency shift between the extrema of the PP signal should closely correspond to the value of the anharmonicity.

As one can see in Fig.6.5c, the linear absorption spectrum of H_2O in acetonitrile in the studied spectral region consists of two bands. This is due to the fact that a H_2O molecule is a typical example of a molecule with the symmetry type C_{2V} [38], where the stretching vibration is delocalized over two bonds and consequently split into two modes: symmetric and antisymmetric. The energy difference between these modes in the case of water is about 90 cm^{-1}. The absorption peak of the antisymmetric vibrational mode is at 3635 cm^{-1}, while the absorption corresponding to the symmetric mode peaks at 3545 cm^{-1}. As a result of such intramolecular delocalization of the vibrational mode, the structure of the pump-probe signal for this sample is more complex than in the case of HDO molecules, where the OH-stretch vibration is mostly localized on the OH-bond. Taking into account a relatively small energy difference between the symmetric and antisymmetric vibrations, these modes can interact with each other leading to the appearance of cross terms [39]. The transitions from the excited state of the symmetric stretching mode to the second excited state of the antisymmetric stretching

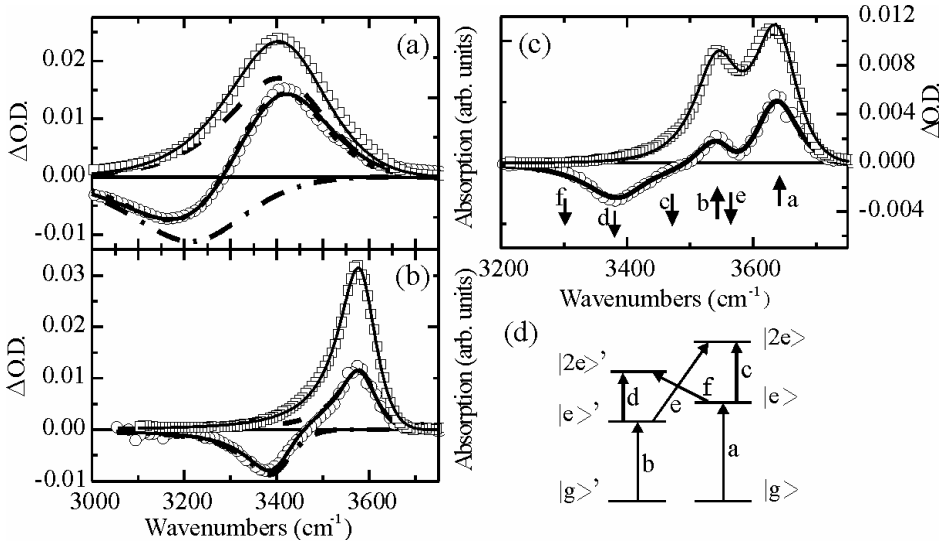

Fig.6.5. Frequency resolved pump-probe signals (circles) and linear absorption spectra (squares) for solutions of HDO in D_2O (a), HDO in acetonitrile (b) and H_2O in acetonitrile (c). The thick and thin solid lines represent the simulations of the pump-probe signals and linear absorption spectra, respectively. The dashed and dash-dotted lines in the figures (a) and (b) show the contributions to the pump-probe signal of induced bleaching and induced absorption respectively. The plot (d) represents the energy level scheme and corresponding transitions for H_2O. The arrows in the graph (c) depict the positions of the lines of induced bleaching (pointing upwards) and induced absorption (pointing downwards).

and vice versa are possible in H_2O. The energy absorption diagram for this system is shown in Fig.6.5d. Accordingly, six lines can emerge in the pump-probe signal of this system: two contours of induced bleaching and four of induced absorption. A similar shape of the PP spectrum of H_2O molecules dissolved in methylenechloride was observed earlier [39].

In order to find the frequency shift of the transition $|e\rangle \rightarrow |2e\rangle$ with respect to $|g\rangle \rightarrow |e\rangle$ and the shape of the contour of the excited state transition, we performed the following analysis. The linear absorption and pump-probe spectra were simulated simultaneously in a global fit procedure. It is known that the absorption spectrum of the OH-stretching vibrational mode of water molecules in liquid phase has an asymmetric shape. The asymmetry of the absorption line is determined by the fact that the frequency of this vibration, being strongly influenced by the hydrogen bond, is a nonlinear function of the hydrogen bond length [40,41]. This nonlinearity results in an asymmetric projection of the hydrogen bond fluctuations on the vibrational frequency coordinate. Therefore, the following asymmetric contour – a product of Lorenzian and Gaussian functions - was used to model the lineshape:

$$A(\omega) = H\left[\exp\left(-\frac{1-a}{2}\left(\frac{\omega-\omega_0}{\sigma(1+s(\omega-\omega_0))}\right)^2\right)\right] \Bigg/ \left[1+a\left(\frac{\omega-\omega_0}{\sigma(1+s(\omega-\omega_0))}\right)^2\right] \qquad (6.4)$$

where parameters H, σ, ω_0, s and a define height, width, central frequency, asymmetry and balance between Gaussian and Lorentzian lineshapes, respectively.

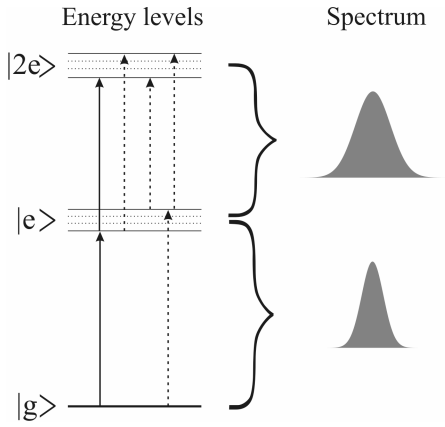

Fig.6.6. Schematic representation of the energy levels, vibrational transitions and resulting spectra for the OH-stretching vibration in HDO molecule.

The linear absorption spectrum and induced bleaching in the pump-probe signal, i.e. the contours that correspond to the transition $|g\rangle \rightarrow |e\rangle$, were fitted with lines having identical shape and position, i.e. parameters $\sigma^{|g\rangle \rightarrow |e\rangle}$, $\omega_0^{|g\rangle \rightarrow |e\rangle}$, $s^{|g\rangle \rightarrow |e\rangle}$ and were global. This is fully justified since no spectral dynamics were observed in the pump-probe signals up to the delay between the pump and probe pulses analyzed here. The induced absorption line had free parameters of height, central frequency and line width.

The results of the fit for the solutions of HDO in heavy water and acetonitrile are presented in Fig.6.5a and b as thick solid lines (total pump-probe signal), thin solid lines (linear absorption spectrum), dashed lines (induced bleaching) and dashed-dotted lines (induced absorption).

For both solutions, the value of the anharmonicity of the OH-stretching vibrational transition in HDO molecules obtained in the fit was 190±20 cm^{-1}. This value acceptably matches the figure derived from the MD simulations for the same system (~185 cm^{-1} [30]). In pure water as well as in acetonitrile solution, the width of the line corresponding to the $|e\rangle \rightarrow |2e\rangle$ vibrational transition, is approximately 1.3-1.5 times larger than the width of fundamental $|g\rangle \rightarrow |e\rangle$ transition. The latter is related to the fact that fluctuations of the fundamental transition ($|g\rangle \rightarrow |e\rangle$) are also projected onto the transition $|e\rangle \rightarrow |2e\rangle$ that leads to increase of the width of the corresponding absorption band in comparison to the spectrum of the ground state transition as illustrated in Fig.6.6. The ratio of heights of the spectral bands corresponding to the transitions $|g\rangle \rightarrow |e\rangle$ and $|e\rangle \rightarrow |2e\rangle$ is close to the harmonic value of 1.4.

The results of the global fit of the linear absorption spectrum and the pump-probe signal for the solution of H_2O in acetonitrile is shown in Fig.6.5c as a solid line. The arrows depict the positions of the respective components, denoted in the energy absorption diagram (Fig.6.5d). The arrows pointing upwards represent the induced bleaching, while those pointing downwards correspond to the induced absorption. For this system, the fit yielded the value of 170±10 cm^{-1} of the anharmonicity of the OH-stretching mode, which also coincides well with the results for HDO molecules. Thus, the anharmonicity of this vibrational mode in HDO and H_2O molecules in pure liquid water as well as in acetonitrile solution, is in the range of 160-210 cm^{-1}**,** which is noticeably lower than the generally accepted value of 270 cm^{-1}.

6.4 Summary and conclusions

Employing broadband IR pulses of 70 fs duration allowed determination of the shape and dynamics of pump-probe spectra with unique accuracy and high spectral and temporal resolution. The quality of the experimental data along with the knowledge of the parameters of the thermal effect that contribute to the experimental pump-probe spectra, provide an opportunity to clarify several important issues related to the ultrafast spectroscopy of water. Namely, the Stokes shift of the spectrum corresponding to the OH-stretch vibration of HDO molecules and the anharmonicity and the shape of the excited state transition absorption band have been elucidated.

In order to provide maximal accuracy in the analysis of the frequency-resolved pump-probe signal dynamics, it was expressed in terms of behavior of the zero crossing wavelength. Analysis of the experimental data showed that within our experimental uncertainty, which does not exceed 5 cm^{-1}, the observed spectral dynamics was related only to the thermal effect – the modifications of the absorption spectrum caused by the heating of the sample due to the absorption of the pump pulse energy. Thus, no appreciable Stokes shift was detected in this system. The absence of a considerable Stokes shift may be related to the fact that the effect of the response of the environment on the average frequency of the excited chromophore is either too weak to be detected with the current technique or occurs on a timescale, which is substantially longer then the population relaxation dynamics. Hence, the stochastic model for the frequency fluctuation correlation function is completely adequate for the description of the interaction of the chromophore with its environment in this system.

Having analyzed the shape of the transient spectra by performing the global fit of the linear absorption and pump-probe spectra, we found that the frequency shift between the transitions $|g\rangle\rightarrow|e\rangle$ and $|e\rangle\rightarrow|2e\rangle$ related to the anharmonicity of the corresponding vibrational mode, amounted to 190±20 cm^{-1}. The width of the line corresponding to $|e\rangle\rightarrow|2e\rangle$ vibrational transition was found to be approximately 1.3-1.5 times larger than the width of fundamental $|g\rangle\rightarrow|e\rangle$ transition, while their height ratio was close to the value 1.4. The frequency-resolved pump-probe experiments on solutions of water in acetonitrile substantiate the validity of our conclusions for pure water.

Appendix 6A

As shown above, the conclusion based on the analysis of the frequency resolved pump experiments, which stated the absence of a significant stokes shift for the OH-stretch vibration of HDO dissolved in D_2O, contradicts the results from Ref.[1]. In the latter study, the Stokes shift of 74 cm^{-1} with a characteristic correlation time of 500 fs was found from the analysis of two-color pump-probe experiments with 200 fs IR pulses. The time-resolved pump-probe transients with spectra of pump and probe pulses positioned consecutively on the blue and red sides of the absorption spectrum were measured in this study. When the spectrum of the pump pulse was tuned on the high-frequency wing of the absorption line, the probe was set at the low frequency side, the time-resolved pump-probe signal appeared with a noticeable delay in respect to the case when the spectra of the pump and probe pulses were positioned in the opposite way. Such behavior of the pump-probe signal was related to the dynamical red shift of the transient absorption spectrum. Therefore, it was interpreted as evidence for the existence of the Stokes shift. The experimental data were analyzed applying the Brownian Oscillator Model in a spectral diffusion limit [42]. The calculations were performed assuming infinitely short excitation pulses (delta-pulse limit). In order to take into account the finite

pulse duration, the authors performed a convolution of the results of the simulations with the experimental cross-correlation function. However, in this way the coherent coupling between the pump and probe pulses is neglected. We will show in this Appendix that the coherent coupling strongly affects the experimental results around the zero delay position, which can lead to a misinterpretation of the experimental data.

We have performed a rigorous theoretical analysis of this case carrying out numerical simulations of the experimental data from the Ref.[1] according to the complete theory expounded in Chapter 3. In this theory all interactions between the pulses are taken into account. The pump-probe signal was calculated for every delay between the excitation pulses as a four-fold integral according to Eq.3.46 (Chapter 3). The response functions (Eqs.3.19-3.22) were modified in order to account for the different central frequencies of the pump and probe pulses in the following way:

$$
\begin{aligned}
&P_A^{(3)}(t,\tau) = \int_0^\infty dt_3 \int_0^\infty dt_2 \int_0^\infty dt_1 \\
&[E_{probe}(t-t_3)E_{pump}(t+\tau-t_3-t_2)E^*_{pump}(t+\tau-t_3-t_2-t_1)R_A^{(1)} + \\
&E_{probe}(t-t_3-t_2)E_{pump}(t+\tau-t_3)E^*_{pump}(t+\tau-t_3-t_2-t_1)R_A^{(2)}]
\end{aligned}
\tag{6.A1}
$$

$$
\begin{aligned}
&R_A^{(1)} = \{\left[\Phi_I(t_1,t_2,t_3)+\Phi_{II}(t_1,t_2,t_3)\right]\times \\
&\exp\left[-i\Delta\omega_{probe}t_3 + i\Delta\omega_{pump}t_1 - 0.5T_1^{-1}(t_3+2t_2+t_1)\right]\} - \\
&r\{\Phi_{III}(t_1,t_2,t_3)\times \\
&\exp\left[-i(\Delta\omega_{TR}+\Delta\omega_{probe})t_3 + i\Delta\omega_{pump}t_1 - 0.5T_1^{-1}(t_3+2t_2+t_1)\right]\}
\end{aligned}
\tag{6.A1a}
$$

$$
\begin{aligned}
&R_A^{(2)} = \{\left[\Phi_I(t_1,t_2,t_3)+\Phi_{II}(t_1,t_2,t_3)\right]\times \\
&\exp\left[-i\Delta\omega_{probe}t_3 + i(\omega_{probe}-\omega_{pump})t_2 + i\Delta\omega_{pump}t_1 - 0.5T_1^{-1}(t_3+2t_2+t_1)\right]\} - \\
&r\{\Phi_{III}(t_1,t_2,t_3)\times \\
&\exp[-i(\Delta\omega_{TR}+\Delta\omega_{probe})t_3 + i(\omega_{probe}-\omega_{pump})t_2 + i\Delta\omega_{pump}t_1 - \\
&0.5T_1^{-1}(t_3+2t_2+t_1)]\}
\end{aligned}
\tag{6.A1b}
$$

$$
\begin{aligned}
&P_B^{(3)}(t,\tau) = \int_0^\infty dt_3 \int_0^\infty dt_2 \int_0^\infty dt_1 \\
&[E_{probe}(t-t_3)E_{pump}(t+\tau-t_3-t_2-t_1)E^*_{pump}(t+\tau-t_3-t_2)R_B^{(1)} + \\
&E_{probe}(t-t_3-t_2-t_1)E_{pump}(t+\tau-t_3)E^*_{pump}(t+\tau-t_3-t_2)R_B^{(2)}]
\end{aligned}
\tag{6.A2}
$$

$$
\begin{aligned}
&R_B^{(1)} = \{\left[\Phi_{IV}(t_1,t_2,t_3)+\Phi_V(t_1,t_2,t_3)\right]\times \\
&\exp\left[-i\Delta\omega_{probe}t_3 - i\Delta\omega_{pump}t_1 - 0.5T_1^{-1}(t_3+2t_2+t_1)\right]\} - \\
&r\{\Phi_{VI}(t_1,t_2,t_3)\times \\
&\exp\left[-i(\Delta\omega_{TR}+\Delta\omega_{probe})t_3 - i\Delta\omega_{pump}t_1 - 0.5T_1^{-1}(t_3+2t_2+t_1)\right]\}
\end{aligned}
\tag{6.A2a}
$$

$$R_B^{(2)} = \{\left[\Phi_{IV}(t_1,t_2,t_3) + \Phi_V(t_1,t_2,t_3)\right]\times$$
$$\exp[-i\Delta\omega_{probe}t_3 + i(\omega_{probe} - \omega_{pump})t_2 - i\Delta\omega_{probe}t_1 - 0.5T_1^{-1}(t_3 + 2t_2 + t_1)]\} -$$
$$r\{\Phi_{VI}(t_1,t_2,t_3)\times \qquad (6\ .A2b)$$
$$\exp[-i(\Delta\omega_{TR} + \Delta\omega_{probe})t_3 + i(\omega_{probe} - \omega_{pump})t_2 - i\Delta\omega_{probe}t_1 - 0.5T_1^{-1}(t_3 + 2t_2 + t_1)]\}$$

$$P_C^{(3)}(t,\tau) = \int_0^\infty dt_3 \int_0^\infty dt_2 \int_0^\infty dt_1$$
$$[E_{probe}(t - t_3 - t_2)E_{pump}(t + \tau - t_3 - t_2 - t_1)E_{pump}^*(t + \tau - t_3)R_C^{(1)} + \qquad (6.A3)$$
$$E_{probe}(t - t_3 - t_2 - t_1)E_{pump}(t + \tau - t_3 - t_2)E_{pump}^*(t + \tau - t_3)R_C^{(2)}]$$

$$R_C^{(1)} = r\{(\Phi_{VIII}(t_1,t_2,t_3)\times$$
$$\exp[-i\Delta\omega_{probe}(t_3 + t_2) - i\,\Delta\omega_{pump}\ t_1 - i(\Delta\omega_{TR} + \Delta\omega_{pump})\,t_2 - 0.5T_1^{-1}(t_3 + t_2 + t_1)]\} -$$
$$r\{\Phi_{VII}(t_1,t_2,t_3)\times \qquad (6.A3a)$$
$$\exp[-i\Delta\omega_{probe}\,t_2 - i\Delta\omega_{pump}\ t_1 - i(\Delta\omega_{TR} + \Delta\omega_{pump})\,t_2 - i(\Delta\omega_{TR} + \Delta\omega_{probe})\,t_3 -$$
$$0.5T_1^{-1}(t_3 + t_2 + t_1)]\}$$

$$R_C^{(2)} = r\{(\Phi_{VIII}(t_1,t_2,t_3)\times$$
$$\exp[-i\Delta\omega_{probe}(t_3 + t_2) - i\Delta\omega_{probe}\,t_1 - i(\Delta\omega_{TR} + \Delta\omega_{pump})\,t_2 - 0.5T_1^{-1}(t_3 + t_2 + t_1)]\} -$$
$$r\{\Phi_{VII}(t_1,t_2,t_3)\times \qquad (6.A3b)$$
$$\exp[-i\Delta\omega_{probe}\,t_2 - i\Delta\omega_{probe}\,t_1 - i\,(\Delta\omega_{TR} + \Delta\omega_{pump})\,t_2 - i\,(\Delta\omega_{TR} + \Delta\omega_{pump})\,t_3 -$$
$$0.5T_1^{-1}(t_3 + t_2 + t_1)]\}$$

$$P_{total}^{(3)}(t,\tau) = P_A^{(3)}(t,\tau) + P_B^{(3)}(t,\tau) + P_C^{(3)}(t,\tau) \qquad (6.A4)$$

where $\Delta\omega_{pump} = \omega_{eg} - \omega_{pump}$, $\Delta\omega_{probe} = \omega_{eg} - \omega_{probe}$, $\Delta\omega_{TR} = \omega_{2ee} - \omega_{eg}$ and the parameter r is introduced to take into account the ratio of the transition dipole moments for the $|g\rangle \rightarrow |e\rangle$ and $|e\rangle \rightarrow |2e\rangle$ transitions. The contributions related to the response functions $R_A^{(1)}, R_B^{(1)}$ and $R_C^{(1)}$ describe the case where the pump pulse precedes the probe, while the terms related to the response functions $R_A^{(2)}, R_B^{(2)}$ and $R_C^{(2)}$ correspond to the opposite situation. The pump-probe signal is then calculated in the following way:

$$S(\Delta\omega_{pump}, \Delta\omega_{probe}, \tau) \propto \int_{-\infty}^{\infty} dt\ \mathrm{Re}\left[E_3^*(t)P_{total}^{(3)}(t,\tau)\right] \qquad (6.A5)$$

In the simulations we used pulses of a ~200 fs duration and a flat spectral phase, which matches the experimental conditions of the experiment described in Ref.[1]. The stochastic model for the molecular dynamics was employed with the following parameters of biexponential correlation function: $1/\Lambda_1$=130 fs, Δ_1=90 cm^{-1}, $1/\Lambda_2$=700 fs, Δ_1=65 cm^{-1}, that

corresponds to the model for the water dynamics presented in Chapters 4. Note, that no Stokes shift is included in this model. The results of our simulations are presented in Fig.6.A1. The upper plot depicts the pump-probe signal (solid line) for the case where the spectrum of the pump pulse is positioned at the blue wing of the absorption line while the probe is at the red side. The laser spectra and the absorption contour are shown in the inset. The dashed line presents the convolution of the cross-correlation of the laser pulses with an exponential function of the form $exp(-t/T_1)$, where T_1=740 fs. This function models instantaneously a raising pump-probe signal. As one can see, the calculated pump-probe is noticeably delayed in respect to the instantaneous signal. At the lower plot, the reversed situation is depicted: the spectrum of the pump is at the red side of the chromophore absorption line, while the probe is at the blue wing. In this case the pump-probe signal (solid line) rises almost simultaneously with the instantaneous signal.

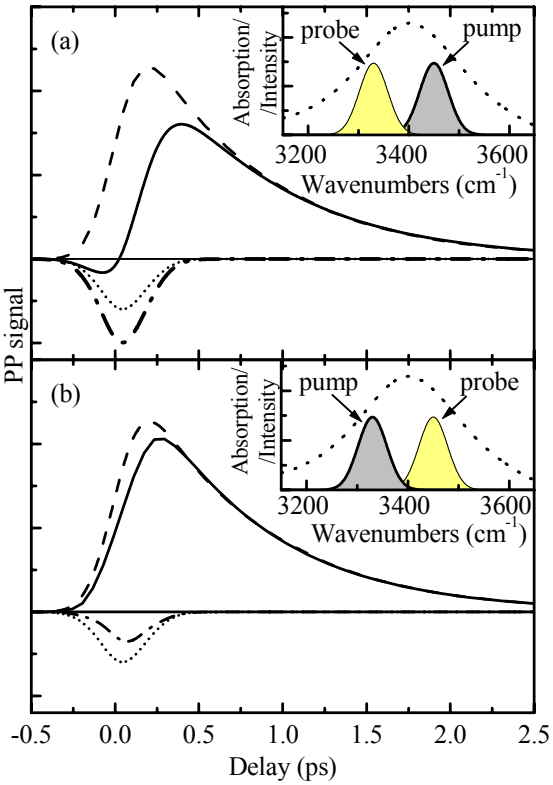

Fig.6.A1. Results of numerical simulations of experimental data from Ref.[1] according to the model described in the text. The solid line represents the calculated pump-probe signal. The dashed line shows instantaneous signal calculated as a convolution of crosscorrelation of pump and probe pulses with an exponential decay function of the form $exp(-t/T_1)$ where T_1=740 fs. The dotted and dash-dotted lines depict the PP signal components related to the response functions $R_A^{(2)}$ and $R_B^{(2)}$ in the case of the 2-level and 3-level systems, respectively. The positions of the spectra of the pump and probe pulses in respect to the absorption line of the OH-stretch vibration of HDO molecules in D_2O are shown in the insets. The pump pulse, probe pulse and the absorption spectrum are depicted by solid, dash-dotted and dotted lines, respectively

Our calculations describe very well the experimental data presented in Ref.[1] without a need to introduce the Stokes shift. Modeling with different contributions to the total pump-probe signal has shown that such initial behavior of the signal is due to coherent interaction of the pump and probe pulses when they exchange their mutual positions in respect to the zero delay point. The contribution related to the response functions $R_A^{(2)}$ and $R_B^{(2)}$, which corresponds to the situation when the probe pulse precedes the pump, is shown in Fig.6A.1 as a short dotted line (2-level system) and a dash-dotted line (3-level system). As one can see, they have a negative sign. If the excited state absorption is not taken into account, (2-level system) the intensity of this signal component does not depend on whether the probe pulse spectrum is positioned at the red or at the blue side of the chromophore absorption band. However, in the realistic 3-level system, where the excited state absorption is considered, the situation is different. When the pump pulse spectrum is on the blue wing of the absorption line, the probe pulse considerably overlaps with the excited state absorption that enhances the signal related to the terms $R_A^{(2)}$ and $R_B^{(2)}$ (dash-dotted line in Fig.6.A1a). When there is an opposite positioning of the pump and probe pulse spectra, this signal component becomes weaker in comparison with the signal in the 2-level model (dash-dotted line in Fig6A.1b). Thus, when the components corresponding to the terms $R_A^{(1)}$, $R_B^{(1)}$ and $R_A^{(2)}$, $R_B^{(2)}$ are summed up, the total signal around the zero delay will be suppressed more in the case when the pump pulse is on the blue wing of the absorption line, than when the position of the laser pulse spectra is the opposite.

References

[1] S. Woutersen, H. J. Bakker. *Phys. Rev. Lett* **83**, 2077 (1999).

[2] W. P. de Boeij: Ultrafast solvation dynamics explored by nonlinear optical spectroscopy., University of Groningen, Groingen, 1997.

[3] M. van Burgel: The ultrafast dynamics of aggregate excitons in water, University of Groningen, Groningen, 1999.

[4] W. P. de Boeij, M. S. Pshenichnikov, D. A. Wiersma. *Ann. Rev. Phys. Chem.* **49**, 99-123 (1998).

[5] G. M. Gale, G. Gallot, F. Hache, N. Lascoux, S. Bratos, J.-C. Leicknam. *Phys. Rev. Lett.* **82**, 1068 (1999).

[6] R. Jimenez, G. R. Fleming, P. V. Kumar, M. Maroncelly. *Nature* **369**, 471-473 (1994).

[7] D. A. Wiersma (Ed.), Femtosecond reaction dynamics. North-Holland, Amsterdam, 1994.

[8] M. Cho, S. J. Rosenthal, N. F. Scherer, L. D. Ziegler, G. R. Fleming. *J. Chem. Phys.* **96**, 5033-5038 (1992).

[9] S. Bratos, G. M. Gale, G. Gallot, F. Hache, N. Lascoux, J.-C. Leicknam1. *Phys. Rev. E* **61**, 5211-5217 (2000).

[10] S. Yeremenko, M. S. Pshenichnikov, D. A. Wiersma. *Chem. Phys. Lett.* **369**, 107-113 (2003).

[11] J. Stenger, D. Madsen, P. Hamm, E. T. J. Nibbering, T. Elsaesser. *Phys. Rev. Lett.* **87**, 027401 (2001).

[12] J. L. Green, A. R. Lacey, M. G. Sceats. *J. Phys. Chem.* **90**, 3958-3964 (1986).

[13] D. E. Hare, C. M. Sorensen. *J. Chem. Phys.* **93**, 6954 (1990).

[14] D. E. Hare, C. M. Sorensen. *J. Chem. Phys.* **96**, 13-22 (1992).
[15] Y. Marechal. *J. Chem. Phys.* **95**, 5565-5573 (1991).
[16] W. B. Monosmith, G. E. Walrafen. *J. Chem. Phys.* **81**, 669-674 (1984).
[17] M. Moskovits, K. H. Michaelian. *J. Chem. Phys.* **69**, 2306-2311 (1978).
[18] W. F. Murphy, H. J. Bernstein. *J. Phys. Chem.* **76**, 1972 (1972).
[19] J. R. Reimers, R. O. Watts. *Chem. Phys. Lett.* **94**, 222-226 (1983).
[20] G. E. Walrafen, M. S. Hokmabadi, W.-H. Yang. *J. Chem. Phys.* **85**, 6964 (1986).
[21] G. E. Walrafen. *J. Chem. Phys.* **48**, 244-251 (1968).
[22] G. E. Walrafen. *J. Chem. Phys.* **47**, 114-127 (1967).
[23] M. Falk, T. A. Ford. *Can. Journal of Chem.* **44**, 1699-1707 (1966).
[24] F. O. Libnau, J. Toft, A. A. Christy, O. M. Kvalheim. *J. Am. Chem. Soc.* **116**, 8311 (1994).
[25] H. J. Bakker, H.-K. Nienhuys, G. Gallot, N. Lascoux, G. M. Gale, J.-C. Leicknam, S. Bratos. *J. Chem. Phys.* **116**, 2592-2598 (2002).
[26] H. J. Bakker, S. Woutersen, H.-K. Nienhuys. *Chem. Phys.* **258**, 233-245 (2000).
[27] H.-K. Nienhuys, S. Woutersen, R. A. van Santen, H. J. Bakker. *J. Chem. Phys.* **111**, 1491 (1999).
[28] H.-K. Nienhuys, R. A. van Santen, H. J. Bakker. *J. Chem. Phys.* **112**, 8487-8494 (2000).
[29] S. Woutersen, U. Emmerichs, H.-K. Nienhuys, H. J. Bakker. *Phys. Rev. Lett.* **81**, 1106 (1998).
[30] C. P. Lawrence, J. L. Skinner. *J. Chem. Phys.* **117**, 8847-8854 (2002).
[31] J. Stenger, D. Madsen, P. Hamm, E. T. J. Nibbering, T. Elsaesser. *J. Phys. Chem. A* **106**, 2341-2350 (2002).
[32] H. Graener, G. Seifert, A. Laubereau. *Phys. Rev. Lett.* **66**, 2092 (1991).
[33] H. J. Bakker, H.-K. Nienhuys. *Science* **297**, 587-590 (2002).
[34] J. C. Deak, S. T. Rhea, L. K. Iwaki, D. D. Dlott. *J. Phys. Chem. A* **104**, 4866-4875 (2000).
[35] D. D. Dlott. *Chem. Phys.* **266**, 149-166 (2001).
[36] A. von Jena, H. E. Lessing. *Appl. Phys.* **19**, 131-144 (1979).
[37] J. E. Bertie, Z. Lan. *J. Phys. Chem. B* **101**, 4111-4119 (1997).
[38] G. Herzberg: Infrared and Raman Spectra of Polyatomic Molecule, Krieger, New York, 1991.
[39] H. Graener, G. Seifert. *J. Chem. Phys.* **98**, 36-45 (1993).
[40] W. Mikenda. *J. Mol. Structure* **147**, 1-15 (1986).
[41] C. P. Lawrence, J. L. Skinner. *Chem. Phys. Lett.* **369**, 472-477 (2003).
[42] S. Mukamel: Principles of Nonlinear Optical Spectroscopy, Oxford University Press, New York, 1995.